Published in final edited form as:
Radiat Res. 2010 August ; 174(2): 216–227. doi:10.1667/RR1866.1.

Investigation of Adaptive Responses in Bystander Cells in 3D Cultures Containing Tritium-Labeled and Unlabeled Normal Human Fibroblasts

Massimo Pinto[1], **Edouard I. Azzam**, and **Roger W. Howell**[2]
Department of Radiology, Division of Radiation Research, UMDNJ - New Jersey Medical School Cancer Center, Newark, New Jersey 07103

Abstract

The study of radiation-induced bystander effects in normal human cells maintained in three-dimensional (3D) architecture provides more *in vivo*-like conditions and is relevant to human risk assessment. Linear energy transfer, dose and dose rate have been considered as critical factors in propagating radiation-induced effects. This investigation uses an *in vitro* 3D tissue culture model in which normal AG1522 human fibroblasts are grown in a carbon scaffold to investigate induction of a G_1 arrest in bystander cells that neighbor radiolabeled cells. Cell cultures were co-pulse-labeled with [^{3}H]deoxycytidine (^{3}HdC) to selectively irradiate a minor fraction of cells with 1–5 keV/μm β particles and bromodeoxyuridine (BrdU) to identify the radiolabeled cells using immunofluorescence. The induction of a G_1 arrest was measured specifically in unlabeled cells (i.e. bystander cells) using a flow cytometry-based version of the cumulative labeling index assay. To investigate the relationship between bystander effects and adaptive responses, cells were challenged with an acute 4 Gy γ-radiation dose after they had been kept under the bystander conditions described above for several hours, and the regulation of the radiation-induced G_1 arrest was measured selectively in bystander cells. When the average dose rate in ^{3}HdC-labeled cells (<16% of population) was 0.04–0.37 Gy/h (average accumulated dose 0.14–10 Gy), no statistically significant stressful bystander effects or adaptive bystander effects were observed as measured by magnitude of the G_1 arrest, micronucleus formation, or changes in mitochondrial membrane potential. Higher dose rates and/or higher LET may be required to observe stressful bystander effects in this experimental system, whereas lower dose rates and challenge doses may be required to detect adaptive bystander responses.

INTRODUCTION

For many decades, the central tenet of radiation biology was that the biological effects of ionizing radiation occur only in cells that are directly hit by radiation. In the last decade, evidence has emerged regarding radiation-induced bystander effects, which are generally defined as detrimental or protective biological effects in unirradiated cells produced by signaling from irradiated neighboring cells (1). Such signals are believed to be propagated either via gap junctions, via secreted diffusible factors, or via a mechanism involving signaling from the plasma membrane (2–5). Oxidative metabolism also appears to be a regulator of both bystander effects and other non-(DNA)-targeted effects of low-dose radiation (6). Several laboratories have reported bystander cell killing, mutations, neoplastic

[2]Address for correspondence: Division of Radiation Research, UMDNJ - New Jersey Medical School, NJMS Cancer Center, F1208, 205 S. Orange Ave., Newark, NJ 07103; rhowell@umdnj.edu.
[1]Present address: Institute of Metrology of Ionizing Radiation, INMRI-ENEA CR Casaccia, Via Anguillarese, 301, S. M. Galeria, I-00060 Rome, Italy.

transformation, chromosome aberrations, DNA damage, induction of micronuclei, apoptosis and induction of differentiation (7–9). While these effects were mainly observed after exposure to high-linear energy transfer (LET) radiations, they were also observed after low-LET radiation exposures (10). Although bystander effects may share similarities with effects caused by direct exposure to ionizing radiation, the molecular fingerprint of damage induced under bystander conditions suggests that mechanisms may be involved that differ from those that follow direct radiation exposure (11–13). Thus, while the phenomenology of radiation-induced bystander effects is well established, the underlying molecular/biochemical events are not fully understood (3,14). Elucidation of these events may affect both radiation protection and radiation therapy of cancer (1,15–19).

Another phenomenon of low-dose radiobiology is the adaptive response, which has been observed both *in vivo* and *in vitro*[3] (20,21). *In vitro*, cells become more resistant to a challenge dose of ionizing radiation if they have been pretreated with a small conditioning dose some time earlier. Early evidence of an adaptive response was demonstrated using a low-dose-rate conditioning dose that was delivered with intracellularly incorporated tritiated thymidine ([^{3}H]dThd) (20). Many studies have been carried out with low conditioning doses (of the order of 1 cGy) delivered acutely or chronically with external beams of mainly low-LET ionizing radiations.

Emerging evidence points to phenomenological connections between the adaptive response and the bystander effect induced by ionizing radiation (14,17,22,23). It is now evident that unirradiated bystander cells may react to a challenge dose as if they had been conditioned, though the conditioning agent was not direct radiation exposure but the consequences of intercellular bystander signaling (24–26). Conversely, a conditioning low dose of radiation may abolish the stressful bystander effect (28,29). It is conceivable that the emerging links between bystander effects, adaptive responses and radiation-induced genomic instability may enrich our overall understanding of low-dose radiation biology (17,29).

It is preferred that an experimental model for studying bystander effects offer unequivocal identification of irradiated and unirradiated cells, leaving both classes of cells minimally perturbed by the identification process. To address this *in vitro*, many strategies have been adopted, including single-cell irradiation with charged-particle microbeams and soft X-ray microprobes (30–33), growth medium transferred from irradiated to unirradiated cells (34) or shared in a transwell coculture system (5,35), and exposure to low fluences of α particles, where only a small fraction of cells are irradiated (36,37). Other approaches have been developed in which cells labeled with tritium that is incorporated into the DNA are tagged with fluorochromes for later identification, mixed with unlabeled cells (bystanders), and assembled as either 2D or 3D cocultures, whereby only the radiolabeled cells experience a significant radiation insult (38–42). *In vitro* and *ex vivo* 3D experimental models have attracted particular attention in recent years, thanks to their potential to fill the gap between *in vitro* 2D models and *in vivo* models, while retaining tight control over experimental variables (40,43–46). A specific limitation in assembling radiolabeled and unlabeled cells as cocultures is that, by the time intercellular communication is established, the effects of any early intercellular signaling events may be missed. Also, in coculture of rapidly mixed populations, the 3D extracellular environment may be poorly representative of the tissue environment, which is believed to be a key modulator of intercellular communication and to affect most aspects of cell behavior (47–50).

[3]E. I. Azzam, Adaptive responses to ionizing radiation in normal human skin fibroblasts. Carleton Institute of Biology, University of Ottawa, Ottawa, 1994.

Building on our previous work with the 3D *in vitro* Cytomatrix™ model (40,46), we report here on the bystander effect, and its adaptive-like behavior, induced by irradiation with low-energy electrons from β-particle decay of tritiated deoxycytidine (^{3}HdC) incorporated in the DNA of human skin fibroblasts that were cocultured with unlabeled cells (bystander cells). Identification of radiolabeled cells is facilitated by dual pulse-labeling with ^{3}HdC and the thymidine analog bromodeoxyuridine (BrdU), whose incorporation in the DNA of radiolabeled cells can be revealed via immunofluorescence, at a dose that does not appear to perturb the biological system (51). The induction of a stress-related G_1 arrest was measured in bystander cells using a flow cytometry-based cumulative labeling index assay (51). To investigate the relationship between the adaptive response and the bystander effect in this biological model, the induction of a G_1 arrest by an acute dose of γ radiation was measured in cells that had been maintained previously in bystander conditions as 3D cocultures with ^{3}HdC-labeled cells. To support the measurements made at the level of the G_1 arrest, the involvement of DNA damage in the responses observed was investigated specifically in bystander cells using an immunofluorescence-based modification of the cytochalasin block micronucleus assay. Oxidative stress in mitochondria was also evaluated by measuring the mitochondrial membrane potential (52).

METHODS

Cell Culture

AG1522 human skin fibroblasts were obtained from the Coriell Cell Repository (Camden, NJ). Cells at passage 11 were cultured in minimum essential medium (Cellgro) supplemented with inactivated 12.5% v/v fetal bovine serum (FBS, Nova Cell), 100 U/ml penicillin and 100 ng/ml streptomycin (Cellgro), and 2 m*M* L-glutamine (Invitrogen). This complete medium preparation is designated cMEM. Cultures were maintained at 37°C as described previously (46). Cells were grown in three dimensions on Cytomatrix™ carbon units (Cell Sciences PTE, Singapore) coated with FNC Coating Mix® reagent containing fibronectin, collagen and albumin (Athena Environmental Sciences). The Cytomatrix™, a highly porous and biocompatible scaffold, is made entirely of carbon and allows cells to grow in 3D as in the body (53). The carbon skeleton is made by pyrolysis of common thermosetting foams. The open cellular geometry of the foam, which is organized as an array of continuously interconnected dodecahedrons with no dead space, makes the scaffold ideal for cell growth. Pore diameters vary from 100–300 μm, and cultures tend to adhere initially on the carbon surface and then multiply inward toward the centers of the cavities (Fig. 1A). At the initial stages of growth, single cells were often observed under a microscope to stretch across an entire cavity and adhere to its opposed walls. To ensure that measurements in 3D cultures were not contaminated by any 2D cultures growing on the surface of culture dishes, Cytomatrices were maintained in 1 ml of cMEM in 24-well plates that were treated to prevent cells from adhering to plastics (Corning). 3D cultures were allowed to move gently on a nutator (Clay Adams) while inside the incubator. cMEM was replaced at varying intervals depending on the radiolabeling conditions (see below).

To obtain single cell suspensions for analyses, cells grown on Cytomatrices were washed twice with 1× Hanks' balanced salt solution (HBSS) at 37°C before treatment with trypsin/EDTA 0.25% w/v (Cellgro) for 2–3 min at room temperature to dismantle the 3D cultures. When 1×10^5 cells were inoculated on each matrix unit, approximately 5×10^5 cells were harvested into a single cell suspension.

Characterization of the Cell Cycle Distribution of the 3D Culture

To set up the Cytomatrix™ bystander model, the cell cycle distribution of 3D cultures was characterized as a function of the schedule of feeding with fresh medium. A total of 1×10^5

cells were inoculated on each FNC-coated Cytomatrix™ unit in 24-well plates with 1 ml cMEM per well. A total of 1×10^5 cells were also seeded in T-25 flasks as a 2D growth control. 2D and 3D cultures were fed every 24 or 48 h (30 min) for 12 days. At 24-h intervals, cultures were harvested by trypsinization, centrifuged and resuspended in PBS, fixed in 70% EtOH, treated with DNase-free RNase (Sigma R4642, 117 Kunitz units/ml) and 50 μg/ml propidium iodide (PI, Fluka), subjected to flow cytometry with fluorescence acquired after 585 ± 42 nm filtration, and subjected to DNA content analysis using the DNA histogram fitting algorithms in the ModFit package (Verity Software, version 3). The cell cycle distribution of each sample was evaluated. Discrimination of cell doublets was achieved by simultaneous analysis of area and width of the electronic signal associated with PI fluorescence (55).

Creation of Bystander Conditions

Solutions of 10 μ*M* BrdU (Sigma) were prepared in cMEM. 2′-Deoxycytidine (5-^{3}H(N), Moravek Biochemicals) was obtained at an activity concentration of 37 MBq/ml and specific activity 855 GBq/mmol. This was diluted in cMEM to an activity concentration of 185 kBq/ml and deoxycytidine concentration of 0.21 μ*M*. AG1522 cells were grown on a Cytomatrix™ for 10–13 days before dual pulse labeling with 185 kBq/ml (0.21 μ*M*) ^{3}HdC and 10 μ*M* bromodeoxyuridine. A pulse of 3 h was followed by six washes with fresh, warm cMEM (total washing time 30 min). Cells were briefly incubated between each wash, and after washes, incubation times varied from a few hours to 2 days, depending on the assay. This pulse-labeling procedure results in a small fraction of cells that are labeled with ^{3}HdC (Fig. 2) and therefore chronically irradiated internally with β particles until the time of assay. Cellular uptake of radioactivity and the absorbed dose to the cell nucleus were determined as described previously (47). Because of the extremely short range of the β particles, neighboring cells are not significantly irradiated and therefore may be considered bystander cells (41,55).

Under the radiolabeling conditions described above, all cells are irradiated by β particles emitted by ^{3}HdC in the culture medium during the 3-h pulse-labeling period. Assuming that the intracellular ^{3}HdC concentration is the same as the ^{3}HdC concentration in the extracellular cMEM (185 kBq/ml), the equilibrium dose constant $\Delta = 9.08 \times 10^{-16}$ Gy kg Bq^{-1} s^{-1} (56) can be used to calculate this dose rate during the pulse-labeling period, which is 0.6 mGy/h. To ensure that this low-dose-rate, low-LET irradiation does not cause a measurable biological effect in unlabeled cells, additional experiments with external chronic γ irradiation at matched low dose rate were conducted, assuming isoeffectiveness with irradiation by β particles emitted by unincorporated ^{3}HdC.

External-Beam Irradiations

External chronic γ irradiation of 3D cultures was conducted at low dose rate (0.6 mGy/h) in a temperature-controlled box at 37°C in a ^{137}Cs γ irradiator (J. L. Shepherd, Model 28-8) (57). External acute γ irradiation of 3D cultures was carried out at room temperature with a ^{137}Cs-irradiator at a dose rate of 1.37 Gy/min (J. L. Shepherd, Mark I). Cells were harvested by trypsinization immediately after irradiation.

Flow Cytometry-Based Cumulative Labeling Index Assay

The flow cytometry-based adaptation of the cumulative labeling index assay was designed to measure the induction of G_1 arrest specifically in bystander cells that are cocultured with ^{3}H-labeled cells while concomitantly measuring both levels of incorporated radioactivity in individual labeled cells and their radiation-induced G_2 arrest (51). Briefly, after cells were dual pulse labeled with ^{3}HdC and BrdU and held in 3D Cytomatrix™ cultures for various times as described above, the cells were harvested with trypsin and

cultured in P60 dishes under subconfluent conditions in cMEM supplemented with 1 μ*M* iododeoxyuridine (IdU, Fluka). At regular times thereafter, cells were harvested by trypsinization, fixed in 70% ethanol and subjected to immunofluorescence with a highly specific antibody against BrdU (#ab6326, AbCam) to identify radiolabeled or sham-labeled cells and an antibody that reacts with both BrdU and IdU (Becton Dickinson) to measure IdU incorporation. To determine the labeling indices of the cells harvested from the cultures, samples were subjected to multiparameter flow cytometry with 488-nm and 633-nm excitation wavelengths (Ar and He-Ne Laser, respectively). IdU incorporation was determined specifically among $BrdU^-$ events (as revealed with the anti-BrdU specific antibody) that registered positives to the anti-BrdU/IdU antibody. Concomitantly, a radiation-induced G_2 arrest was measured in $BrdU^+$ cultures using DNA histogram analysis as described previously (46,51).

Micronucleus/BrdU Immunofluorescence Assay

Cells harvested from Cytomatrices were cultured for 72 h in two or four multiwell slide chambers (Nalgene Nunc) with 2.0 μg/ml Cytochalasin B (Sigma) in cMEM. For microscopic observation of micronuclei, cells adhering to the slide chambers were fixed with 70% EtOH for 2 min, rinsed with distilled water, and subjected to immunodetection of BrdU to measure micronuclei in $BrdU^-$ or $BrdU^+$ cells. To this end, the protocol of Schutte *et al.* was adopted (58) with some modifications. Samples were first treated for 15 min at 37°C with 2N HCl and 0.2 mg/ml pepsin (Sigma), then neutralized with 1 *M* Tris-HCl, pH 10.0. Cells were washed with 1% w/v BSA in PBS (Promega) and reacted with 1:50 rat anti-BrdU (#ab6326 AbCam) in 0.5% v/v Tween 20 (Sigma), 1% FBS, in 1% w/v BSA (designated Ab buffer) for 25 min at room temperature. After washing with BSA solution, cells were immunoreacted with Alexa 568-conjugated anti rat (Invitrogen) secondary antibody diluted to 1:5000 in Ab buffer for 25 min at room temperature. Samples were finally washed with BSA solution and covered with 5 μl Hoechst 33342 at 1:5000 dilution in water, mounted with cover slips, and viewed under a microscope at 400× magnification. Slides were coded, and micronucleus events were scored separately according to BrdU content using the criteria described in ref. (59). Cells with nucleoplasmic bridges were not scored, and cells that contained both micronuclei and nucleoplasmic bridges were counted as micronucleated events. The number of binucleate events scored for each treatment condition in every experiment ranged from 1000 to 2000 cumulated from duplicate samples. Sample digital images were captured with a black and white CCD camera (Olympus) on an Olympus IX70 inverted fluorescence microscope using a Hoechst/DAPI filter cube set and a HQ-TRITC filter cube set (Chroma). Black and white digital pictures acquired in separate color channels were then assigned a pseudo color for illustrations.

Mitochondrial Membrane Potential

For some experiments, parallel Cytomatrix™ cocultures of ^{3}HdC/BrdU-labeled and sham-labeled bystander cells were also incubated for 15 min at 37°C in the dark with 1.25 μg/ml lipophilic cation JC-1 probe (Invitrogen-Molecular Probes) dissolved in cMEM. Cultures were then washed with HBSS, harvested with trypsin, resuspended in cMEM, washed with HBSS supplemented with 1.2 m*M* $MgCl_2$ and 0.8 m*M* $CaCl_2$ ($HBSS^+$), and analyzed by flow cytometry on a Becton Dickinson FACSCalibur at 488 nm argon laser excitation. As a positive control of mitochondrial membrane depolarization, cells were grown on separate Cytomatrices and were treated with 10 μ*M* valinomycin (Sigma) dissolved in cMEM for 15 min at 37°C before staining with the JC-1 dye. The depolarization of mitochondrial membrane was inferred via a shift from red (585 ± 42 nm) to green (530 ± 30 nm) fluorescence and was expressed as the mean ratio of red to green fluorescence in arbitrary units. Unlike the micronucleus and FCM-CLI assays, where the cumulative labeling indices

are determined specifically in bystander cells, the mitochondrial membrane potential was measured in heterogeneous samples containing both radiolabeled (~5%) and unlabeled cells.

Statistical Analysis

Regression analysis of cumulative labeling index data was carried out using the Sigma Plot 10.0 (Systat Software, Inc.) with a sigmoid function. For each independent experiment, the half rise time $X_{0\ Gy}$ was defined as the time when the labeling index of the sham bystander/sham-irradiated sample reached 50% of its maximum. For all other samples (bystander/sham-irradiated, sham bystander/irradiated, and bystander/irradiated) the times at which each corresponding best-fit curve crossed 50% of the sham bystander/sham γ-irradiated maximum was determined ($X_{bystanders}$, $X_{4\ Gy}$, $X_{bystanders,\ 4\ Gy}$, respectively) and the $X_{0\ Gy}$ value was subtracted to estimate the magnitude of any G_1 arrest induced by each treatment (see also Fig. 3A). The X_i estimates were subjected to a paired *t* test and to one-way ANOVA. When the normality test failed, a Mann-Whitney rank sum test was run instead of the *t* test. Micronucleus frequency data and distribution of cumulative labeling index experimental outcomes were analyzed for statistical significance using the Pearson χ^2 test on 2 × 2 contingency tables with 1 degree of freedom or 2 × 3 contingency tables with 2 degrees of freedom, respectively. Statistical significance of mitochondrial membrane potential measurements was determined using Student's *t* test. All tests were run using SigmaStat 3.5 (Systat Software).

RESULTS

Design and Development of an Experimental Strategy to Study Bystander Effects in the Cytomatrix™ 3D Culture Model

We first characterized the growth of AG1522 fibroblasts on Cytomatrix™ units. Growth curves were determined first; however, measurements were inexact because a fraction of growing fibroblasts always remained adherent on the Cytomatrix™ units even after trypsinization. Cytomatrix™ cultures were therefore monitored for several days for their distribution through the cell cycle (relative to 2D cultures) by measuring DNA content with flow cytometry at exact 24-h intervals. Percentages of cells in G_2/M, G_0/G_1 and S phase of the cell cycle as a function of time after inoculation are plotted in Fig. 1B–D. The fraction of cells in S phase at a given time is shown in Fig. 1C. A bystander experimental model was obtained by pulse labeling the growing cultures *in situ* with the radiolabeled DNA precursor ^{3}HdC. Only the cells in S phase incorporated ^{3}HdC into their DNA. The nuclei and cytoplasm of the labeled cells were then chronically exposed. The cells that were not labeled with ^{3}HdC (unlabeled) were not significantly irradiated due to the short range of the ^{3}H β particles and were therefore considered bystanders. If cells are cultured in 3C for 10 days before pulse labeling with ^{3}HdC, up to 5% of the cells were in S phase (Fig. 1D) and were available for radiolabeling, the remaining fraction being bystanders distributed throughout all phases of the cell cycle except S. The bystander fraction is composed primarily of G_0/G_1 cells, which closely mimics the condition of several tissues *in vivo*. The fraction of cells in S phase will be enhanced if pulse labeling is carried out 24 h after the last cMEM replacement. In contrast, pulse labeling 48 h after the last feeding results in a minimal labeled fraction. When adopting such a feeding regimen, the complementary G_2/M and G_0/G_1 cell cycle phases display a correspondingly oscillatory behavior (Fig. 1D and B). The G_2/M oscillation in 3D culture is more pronounced than that in 2D (Fig. 1D), although this may vary as function of cell density at inoculation. When cMEM was replaced every day at the same hour, as opposed to every other day, the oscillatory behavior described disappeared (not shown). Furthermore, if cells were maintained in the same cMEM for 72 h before cMEM replacement on day 11, the S-phase fraction on day 12 was higher. The temporal oscillatory cell cycle distribution behavior displayed in Fig. 1B–D also showed a

declining trend that finds its roots in the decreasing percentage of proliferating cells as 2D or 3D confluence is approached.

To obtain highly reproducible labeling and bystander conditions, all experiments were performed with cultures on day 11 and 13, having been fed 24 h earlier and every other previous day. Deviating from the refeeding schedule resulted in an unpredictable fraction of radiolabeled cells, which in some instances reached 15% after a 3-h pulse label. However, even if the fraction of labeled cells was controlled with precision, the actual dose rate to the labeled cells in individual experiments varied significantly, as commonly observed for radionuclide delivery (60).

Bystander and Adaptive Bystander Responses in 3D Cultures: G_1 Arrest

Relative to sham bystander cells (i.e. when BrdU was pulsed without ^{3}HdC), no substantial delay in progression through G_1 phase was detected in bystander cells in most experiments when 3 to 16% of cells cultured on the Cytomatrix™ were radiolabeled with ^{3}HdC to a maximum dose rate of 37 cGy/h. In some experiments, however, a modest bystander effect was evident in the form of a G_1 arrest ($X_{bystanders} > X_{0\ Gy}$), the half-rise value for sham bystander conditions (Table 1), or the induction of faster proliferation ($X_{bystanders} < X_{0\ Gy}$), as shown in Fig. 3A. However, paired *t* tests of the 3-h and 24-h data sets give *P* values of 0.096 and 0.41, respectively, and therefore no significant G_1 arrest was observed in the bystander cells.

When 3D cocultures of ^{3}HdC-labeled and unlabeled cells (bystanders) were held for 3 or 24 h before being challenged with 4 Gy with acute γ radiation (to evaluate any adaptive bystander response), several cumulative labeling index experiments showed an attenuated G_1 arrest ($X_{bystanders,\ 4\ Gy} < X_{4\ Gy}$) in bystander cells relative to sham bystander cells (Fig. 3A, Table 1). The results of seven of the nine experiments with a 3-h holding time and two of three experiments with a 24-h holding time suggested a modest adaptive bystander effect. However, when the 3-h and the 24-h coculture time sets of cumulative labeling index data were analyzed (Table 1), Student's *t* tests showed that the differences were not statistically significant ($P = 0.16$ and 0.19 for 3 h and 24 h, respectively). Additionally, for the 3-h and the 24-h coculture time data sets, a one-way ANOVA was run on the cumulative labeling indexes for all four treatment groups (sham bystander/sham-irradiated, bystander/sham-irradiated, sham bystander/irradiated, and bystander/irradiated). The ANOVA confirmed that the only statistically significant G_1 arrest was that induced by 4 Gy γ radiation, regardless of pretreatment in 3D bystander conditions ($P < 0.05$).

During the 3-h pulse labeling, all cells, including bystander cells, are exposed to low-dose-rate radiation due to the β particles emitted by unincorporated ^{3}HdC. Therefore, we examined whether such low-dose-rate exposures could explain the modest adaptation of bystander cells (i.e. not ^{3}HdC-labeled) that was seen in some experiments with the 4-Gy challenge γ radiation. FCM-CLI experiments were designed to control for this effect, using external γ irradiation at a matched dose rate (0.6 mGy/h) for 3 h under BrdU pulse-labeling conditions. We found neither induction of a G_1 checkpoint (three experiments, not shown) nor adaptation to a 4-Gy challenge γ irradiation delivered 3 or 24 h later (two experiments), therefore excluding that 1.8 mGy delivered to every cell during the 3 h of the ^{3}HdC/BrdU dual pulse could be responsible for the induction of an adaptive bystander effect at the level of altering the G_1 checkpoint.

Potential Influence of BrdU Incorporation on Bystander Effect Signaling

BrdU is a radiosensitizer when it is incorporated in cellular DNA (61), and the possibility exists that colabeling cells with BrdU and ^{3}HdC could alter the capacity of radiolabeled cells

to send signals to neighboring bystander cells. To test this hypothesis, micronucleus formation was measured in bystander cells when labeled cells contained both BrdU and ^{3}HdC and when they were labeled with ^{3}HdC alone (Fig. 4). We noticed that cells colabeled with BrdU and ^{3}HdC rarely formed any binucleate cells, presumably because they arrested at the G_2/M checkpoint in a dose-dependent fashion [see also flow cytometry measurements in ref. (51)]. Therefore, we determined that only bystander cells were being scored for MN events in samples that were pulsed with ^{3}HdC but not with BrdU. The results showed that the frequency of unlabeled micronucleated cells was not altered by the presence of BrdU in radiolabeled cells, indicating that BrdU incorporation is not a confounding factor for studying ^{3}H-induced bystander effects in this system, at least at the level of induction of micronuclei.

To test whether BrdU incorporation in radiolabeled cells affects the adaptive bystander effect measurements (Fig. 4), 3D cultures that had been pulse-labeled with ^{3}HdC with or without BrdU for 3 h were washed with fresh cMEM six times, incubated in fresh cMEM for 4 h, irradiated acutely with 4 Gy γ rays, harvested by trypsinization, and seeded for micronucleus assay. The results indicated that, under our conditions, coincorporation of BrdU in ^{3}HdC-labeled cells did not alter the frequency of micronucleus induction in bystander cells after irradiation.

DNA Damage: Micronucleus Assay

When cells were harvested after 3, 8 or 24 h of coculture and seeded for micronucleus formation, there were insignificant differences in the percentages of micronucleated binucleate cells in bystander cells relative to those in sham bystander conditions (Fig. 3B, example shown for one experiment). A challenge dose of 4 Gy delivered 3, 8 or 24 h prior to harvesting cells from 3D cultures and assaying for MN induction also resulted in similar micronucleus frequencies in bystander and sham bystander cells (Fig. 3B). The spectrum of micronucleus events after 4 Gy challenge irradiation also showed a similar pattern in sham or bystander cells (one example shown in Fig. 5). Overall, six experiments were subjected to the micronucleus assay (Table 2). The two instances that resulted in significant responses for micronucleus induction did not correlate with observations of G_1 arrest, as measured with the cumulative labeling index assay (Table 1).

Oxidative Stress in Mitochondria

Oxidative stress often results in changes in the membrane potential. The JC-1 probe was used to measure changes in the mitochondrial membrane potential of viable samples [see for example ref. (52)]. Most experiments suggested no changes in membrane potential in the adaptive bystander effect experiments (Table 3 and Fig. 3C). Two experiments (^{3}HdC30 and ^{3}HdC32, Table 3), however, suggested a significant response, but this does not correlate with an observable response at the level of G_1 arrest as assayed via measurement of cumulative labeling index (see experiment ^{3}HdC32 and Table 1).

Summary of Results

In summary, the results suggest that low-dose-rate (<37 cGy/h) β-particle irradiation by DNA-incorporated ^{3}HdC does not induce a G_1 arrest in bystander cells in our 3D Cytomatrix™ cultures. Compared to sham bystander conditions, bystander cells respond to a challenge 4-Gy γ irradiation with a slightly shorter but not statistically significant G_1 arrest. This may suggest a modest adaptive bystander effect, but it did not correlate with the response to DNA damage or with oxidative stress as reflected by alterations in mitochondrial membrane potential.

DISCUSSION

Here we describe the design and the implementation of a novel approach to study the radiation-induced bystander effect in a 3D *in vitro* culture system that uses normal human fibroblasts at 37°C. In this system, cells are labeled with tritiated deoxycytidine (^{3}HdC) while being cocultured in 3D with bystander cells. Coculturing ^{3}H-labeled and unlabeled cells provides a valuable tool to investigate bystander effects caused by exposure to β particles from tritium (38,46,51,62). One distinct characteristic of the Cytomatrix™ model described here is that radiolabeling occurs *in situ*, when the 3D cultures are already assembled with presumably functional gap junctions and a structural/functional extracellular matrix, which is known to be secreted by fibroblasts. This allows early bystander signaling and the consequent signal transduction that may play a role in the biological responses that are being measured. This is a distinct advantage over prelabeling with radiopharmaceuticals and fast assembly of cocultures with bystander cells. A drawback of the *in situ* labeling strategy is that, to enhance incorporated radioactivity in labeled cells, an unwanted low dose must be imparted to the entire culture during labeling due to the presence of ^{3}HdC molecules in the labeling medium. While the effects of this unwanted low-dose irradiation were controlled for by additional experiments, it may need to be considered if the dose rate to the targeted cells is increased substantially. A second inconvenience of the approach is that BrdU, a known radiosensitizer, is incorporated concomitantly with ^{3}HdC. However, our control studies suggested that coincorporation of BrdU did not interfere with our assays (Fig. 4).

Under our Cytomatrix™ culture conditions wherein a small fraction of the cells are labeled with ^{3}HdC, we found no significant bystander responses for induction of a G_1 arrest, no elevation of micronucleus frequency, and no alterations in mitochondrial membrane potential when the radiolabeled cells were being irradiated at dose rates up to 37 cGy/h (Fig. 3 and Table 1). A modest adaptive bystander effect was observed in several experiments as an attenuated G_1 arrest after a challenge dose of 4 Gy γ rays that was delivered several hours after bystander conditions were established in 3D cocultures (Table 1). Statistical analyses of grouped experiments indicated, however, that the effect was not statistically significant. It cannot be excluded that a statistically significant adaptive bystander effect could be observed if a challenge dose smaller than 4 Gy were used.

The cytochalasin-block micronucleus experiments, measuring a surrogate marker of DNA damage, showed no DNA damage under the bystander conditions used here. Also, as indicated by parallel measurements of micronuclei induced by a challenge dose of 4 Gy γ radiation, the micronucleus frequencies were not altered by earlier bystander culture conditions (Fig. 3B and Table 2). Similarly, the micronucleus frequency distribution in bystander cells, which may be indicative of complexity of DNA damage induced by 4 Gy γ radiation, appeared to be unaltered by bystander conditions (Fig. 4C). Iyer and Lehnert, in a medium transfer model also using human fibroblasts, found a role for DNA repair in adaptive bystander effects after γ irradiation, as indicated by up-regulation of the DNA repair protein AP-endonuclease (24,25). Oxidative metabolism has also been implicated as a regulator of bystander signaling/response (6). However, under the conditions we used, and consistent with the lack of manifestation of bystander effects with the other two assays that were used, oxidative metabolism at the level of mitochondria did not appear to be involved (example in Fig. 3C).

Any bystander signaling in our experiments would have been initiated by radiolabeled cells that became synchronized in G_2 phase as a consequence of a G_2/M arrest induced by ^{3}H decays in the DNA (46,51). Studies from other laboratories suggest that growth-inhibited cells, synchronized in G_0 phase, including AG1522 fibroblasts, manifest the capacity to

signal bystander effects (2,63), a feature that is also ascribed to exponentially growing cultures (64). Our results may suggest that the capacity of AG1522 fibroblasts to signal bystander responses is limited when the labeled cells are synchronized in G_2 phase.

There may be several other reasons why we did not observe a statistically significant bystander effect in our experiments. One may be the novelty of the model itself: although the bystander effect in AG1522 cells is documented in two-dimensional cultures (2,10) exposed to high-LET α particles, this appears to be the first study published to date using the AG1522 cell strain in a 3D culture environment and with an *in situ* radiolabeling strategy. However, pilot 2D experiments using a similar labeling strategy yielded similar results (not shown). Cell culture architecture was shown to result in different expression of Connexin 43 and regulation of G_1 arrest in this cell strain in our laboratory (65) However, the expression level of Connexin 43, one of the gap junction proteins involved with detrimental bystander signaling (66), was higher. Therefore, one would expect that bystander effects would be more prominent in 3D than 2D. The dose rate used here was never higher than 37 cGy/h and was in a relatively low-dose-rate region. Other studies on bystander killing signaled from tritium-labeled cells showed a marked dose-dependent effect (40–42). However, although they used a radically different cell culture model, Persaud *et al.* showed that even low doses delivered by DNA-incorporated tritium can induce mutations in neighboring bystander cells (42). Other studies indicate that the effect may be propagated to bystander cells only if the ratio of labeled to unlabeled cells in the coculture exceeds a threshold (39). Thus our labeling of only 5% of the cells may be insufficient to elicit a bystander response. This last feature may be different in experiments with targeted microbeams, where effects are observed after irradiation of a single cell (64). A more prominent bystander effect might have been detected in our model had the dose rate to the labeled cells been higher or if more cells had been targeted or both. Supporting this hypothesis are our results using tritium and AG1522 cells showing that a dose-rate threshold may have to be reached before bystander signaling and/or response is measurable (Azzam *et al.*, in preparation). The dose delivered to the cells signaling the bystander effect may also determine the character of the bystander response, as highlighted by Iyer and Lehnert, who showed that the effect differed for doses to the bystander-signaling cells of 1 cGy and 1 Gy (24). Earlier experiments with accelerated ^{4}He particles of high LET showed that two nuclear traversals were sufficient to induce neoplastic transformation in bystander cells (67) and that, for cell killing, the effect increased with more particle traversals (68), indicative of a dose dependence for the magnitude of the bystander response. Single hits by high-LET particles have also been shown to impart doses large enough to trigger bystander signals (36); these doses cannot be attained after a single electron traversal. In contrast, another recent study reported a binary, switch-like behavior in which the magnitude of the effect did not appear to depend on the radiation dose to the targeted cells; in particular, an irradiated cell may or may not send a stressful bystander signal with a probability of doing so that is proportional to the dose when it is below 0.3 Gy (64). In early adaptive response studies, tritium-labeled lymphocytes cultured in suspension did not appear to impart bystander responses in unlabeled cells (21).

In conclusion, ^{3}H-deoxycytidine selectively incorporated into the DNA of only about 5% of AG1522 cells growing three-dimensionally in a Cytomatrix™ did not appear to induce statistically significant bystander or adaptive bystander responses as measured by perturbations in the G_1 checkpoint, induction of micronuclei, and changes in mitochondrial membrane potential. The continuously emerging phenomenological picture of bystander effects clearly depends on the culture model as well as the experimental design. With respect to human risk estimates, it is paramount to encourage future investigations in experimental bystander models that increasingly mimic the human scenario *in vivo*.

Acknowledgments

We thank P. Neti, M. Buonanno, S. M. de Toledo, B. Pandey, P. Venkatachalam, N. Asaad and B. I. Gerashchenko for their constructive criticism. The project described was supported in part by Grants 2R01 CA83838 (RWH) and 1R01 CA92262 (EIA) from the National Cancer Institute. The content is solely the responsibility of the authors and does not necessarily represent the official views of the National Cancer Institute or the National Institutes of Health. The project was also supported in part by a New Jersey Commission for Cancer Research Post Doctoral Fellowship (MP) and a UMDNJ Foundation Scholarship (MP).

References

1. Wright EG, Coates PJ. Untargeted effects of ionizing radiation: implications for radiation pathology. Mutat Res 2006;597:119–132. [PubMed: 16438994]
2. Azzam EI, de Toledo SM, Gooding T, Little JB. Intercellular communication is involved in the bystander regulation of gene expression in human cells exposed to very low fluences of alpha particles. Radiat Res 1998;150:497–504. [PubMed: 9806590]
3. Little JB. Cellular radiation effects and the bystander response. Mutat Res 2006;597:113–118. [PubMed: 16413041]
4. Nagasawa H, Cremesti A, Kolesnick R, Fuks Z, Little JB. Involvement of membrane signaling in the bystander effect in irradiated cells. Cancer Res 2002;62:2531–2534. [PubMed: 11980645]
5. Gerashchenko BI, Howell RW. Cell proximity is a prerequisite for the proliferative response of bystander cells co-cultured with cells irradiated with gamma-rays. Cytometry 2003;56A:71–80. [PubMed: 14608634]
6. Azzam EI, de Toledo SM, Little JB. Oxidative metabolism, gap junctions and the ionizing radiation-induced bystander effect. Oncogene 2003;22:7050–7057. [PubMed: 14557810]
7. Azzam EI, de Toledo SM, Little JB. Stress signaling from irradiated to non-irradiated cells. Curr Cancer Drug Targets 2004;4:53–64. [PubMed: 14965267]
8. Goldberg Z, Lehnert BE. Radiation-induced effects in unirradiated cells: a review and implications in cancer. Int J Oncol 2002;21:337–349. [PubMed: 12118330]
9. Belyakov OV, Folkard M, Mothersill C, Prise KM, Michael BD. Bystander-induced differentiation: a major response to targeted irradiation of a urothelial explant model. Mutat Res 2006;597:43–49. [PubMed: 16423374]
10. Yang H, Asaad N, Held KD. Medium-mediated intercellular communication is involved in bystander responses of X-ray-irradiated normal human fibroblasts. Oncogene 2005;24:2096–2103. [PubMed: 15688009]
11. Huo L, Nagasawa H, Little JB. HPRT mutants induced in bystander cells by very low fluences of alpha particles result primarily from point mutations. Radiat Res 2001;156:521–525. [PubMed: 11604065]
12. Nagasawa H, Huo L, Little JB. Increased bystander mutagenic effect in DNA double-strand break repair-deficient mammalian cells. Int J Radiat Biol 2003;79:35–41. [PubMed: 12556329]
13. Chaudhry MA. Bystander effect: biological endpoints and microarray analysis. Mutat Res 2006;597:98–112. [PubMed: 16414093]
14. Azzam EI, Little JB. The radiation-induced bystander effect: evidence and significance. Hum Exp Toxicol 2004;23:61–65. [PubMed: 15070061]
15. Prise KM. New advances in radiation biology. Occup Med (London) 2006;56:156–161. [PubMed: 16641500]
16. Cucinotta FA, Durante M. Cancer risk from exposure to galactic cosmic rays: implications for space exploration by human beings. Lancet Oncol 2006;7:431–435. [PubMed: 16648048]
17. Brooks AL. Paradigm shifts in radiation biology: their impact on intervention for radiation-induced disease. Radiat Res 2005;164:454–461. [PubMed: 16187749]
18. Mothersill C, Seymour CB. Radiation-induced bystander effects—implications for cancer. Nat Rev Cancer 2004;4:158–164. [PubMed: 14964312]
19. Stenerlow B. Radiation-induced bystander effects. Acta Oncol 2006;45:373–374. [PubMed: 16760172]

20. Olivieri G, Bodycote J, Wolff S. Adaptive response of human lymphocytes to low concentrations of radioactive thymidine. Science 1984;223:594–597. [PubMed: 6695170]
21. Wolff S. Is radiation all bad? The search for adaptation. Radiat Res 1992;131:117–123. [PubMed: 1641465]
22. Mothersill C, Seymour C. Radiation-induced bystander effects and adaptive responses—the Yin and Yang of low dose radiobiology? Mutat Res 2004;568:121–128. [PubMed: 15530545]
23. Kadhim MA, Moore SR, Goodwin EH. Interrelationships amongst radiation-induced genomic instability, bystander effects, and the adaptive response. Mutat Res 2004;568:21–32. [PubMed: 15530536]
24. Iyer R, Lehnert BE. Low dose, low-LET ionizing radiation-induced radioadaptation and associated early responses in unirradiated cells. Mutat Res 2002;503:1–9. [PubMed: 12052498]
25. Iyer R, Lehnert BE. Alpha-particle-induced increases in the radioresistance of normal human bystander cells. Radiat Res 2002;157:3–7. [PubMed: 11754635]
26. Maguire P, Mothersill C, McClean B, Seymour C, Lyng FM. Modulation of radiation responses by pre-exposure to irradiated cell conditioned medium. Radiat Res 2007;167:485–492. [PubMed: 17388689]
27. Mitchell SA, Marino SA, Brenner DJ, Hall EJ. Bystander effect and adaptive response in C3H 10T½ cells. Int J Radiat Biol 2004;80:465–472. [PubMed: 15360084]
28. Zhou H, Randers-Pehrson G, Geard CR, Brenner DJ, Hall EJ, Hei TK. Interaction between radiation-induced adaptive response and bystander mutagenesis in mammalian cells. Radiat Res 2003;160:512–516. [PubMed: 14565832]
29. Schwartz JL. Variability: the common factor linking low dose-induced genomic instability, adaptation and bystander effects. Mutat Res 2007;616:196–200. [PubMed: 17145066]
30. Prise, KM.; Folkard, M.; Michael, BD. The use of microbeams in radiation biology: an overview. In: Moriarty, M.; Mothersill, C.; Seymour, C.; Edington, M.; Ward, JF.; Fry, RJM., editors. Proceedings of the 11th International Congress on Radiation Research. Vol. 2. Allen Press; Lawrence, KS: 1999. p. 174-177.
31. Folkard M, Schettino G, Vojnovic B, Gilchrist S, Michette AG, Pfauntsch SJ, Prise KM, Michael BD. A focused ultrasoft X-ray microbeam for targeting cells individually with submicrometer accuracy. Radiat Res 2001;156:796–804. [PubMed: 11741504]
32. Wu LJ, Randers-Pehrson G, Xu A, Waldren CA, Geard CR, Yu Z, Hei TK. Targeted cytoplasmic irradiation with alpha particles induces mutations in mammalian cells. Proc Natl Acad Sci USA 1999;96:4959–4964. [PubMed: 10220401]
33. Schettino G, Folkard M, Prise KM, Vojnovic B, Held KD, Michael BD. Low-dose studies of bystander cell killing with targeted soft X rays. Radiat Res 2003;160:505–511. [PubMed: 14565833]
34. Mothersill C, Seymour C. Medium from irradiated human epithelial cells but not human fibroblasts reduces the clonogenic survival of unirradiated cells. Int J Radiat Biol 1997;71:421–427. [PubMed: 9154145]
35. Shao C, Aoki M, Furusawa Y. Medium-mediated bystander effects on HSG cells co-cultivated with cells irradiated by X-rays or a 290 MeV/u carbon beam. J Radiat Res (Tokyo) 2001;42:305–316. [PubMed: 11840647]
36. Nagasawa H, Little JB. Induction of sister chromatid exchanges by extremely low doses of alpha-particles. Cancer Res 1992;52:6394–6396. [PubMed: 1423287]
37. Azzam EI, de Toledo SM, Little JB. Direct evidence for the participation of gap junction-mediated intercellular communication in the transmission of damage signals from alpha-particle irradiated to nonirradiated cells. Proc Natl Acad Sci USA 2001;98:473–478. [PubMed: 11149936]
38. Gerashchenko BI, Howell RW. Proliferative response of bystander cells adjacent to cells with incorporated radioactivity. Cytometry A 2004;60:155–164. [PubMed: 15290716]
39. Gerashchenko BI, Howell RW. Bystander cell proliferation is modulated by the number of adjacent cells that were exposed to ionizing radiation. Cytometry A 2005;66:62–70. [PubMed: 15915508]

40. Bishayee A, Rao DV, Howell RW. Evidence for pronounced bystander effects caused by nonuniform distributions of radioactivity using a novel three-dimensional tissue culture model. Radiat Res 1999;152:88–97. [PubMed: 10428683]
41. Persaud R, Zhou H, Baker SE, Hei TK, Hall EJ. Assessment of low linear energy transfer radiation-induced bystander mutagenesis in a three-dimensional culture model. Cancer Res 2005;65:9876–9882. [PubMed: 16267011]
42. Persaud R, Zhou H, Hei TK, Hall EJ. Demonstration of a radiation-induced bystander effect for low dose low LET beta-particles. Radiat Environ Biophys 2007;46:395–400. [PubMed: 17554548]
43. Belyakov OV, Folkard M, Mothersill C, Prise KM, Michael BD. A proliferation-dependent bystander effect in primary porcine and human urothelial explants in response to targeted irradiation. Br J Cancer 2003;88:767–774. [PubMed: 12618888]
44. Belyakov OV, Mitchell SA, Parikh D, Randers-Pehrson G, Marino SA, Amundson SA, Geard CR, Brenner DJ. Biological effects in unirradiated human tissue induced by radiation damage up to 1 mm away. Proc Natl Acad Sci USA 2005;102:14203–14208. [PubMed: 16162670]
45. Djordjevic B, Lange CS. Cell-cell interactions in spheroids maintained in suspension. Acta Oncol 2006;45:412–420. [PubMed: 16760177]
46. Pinto M, Azzam EI, Howell RW. Bystander responses in three-dimensional cultures containing radiolabelled and unlabelled human cells. Radiat Prot Dosimetry 2006;122:252–255. [PubMed: 17185313]
47. Barcellos-Hoff MH, Brooks AL. Extracellular signaling through the microenvironment: a hypothesis relating carcinogenesis, bystander effects, and genomic instability. Radiat Res 2001;156:618–627. [PubMed: 11604083]
48. Stevens MM, George JH. Exploring and engineering the cell surface interface. Science 2005;310:1135–1138. [PubMed: 16293749]
49. Mothersill C, Seymour CB. Cell-cell contact during gamma irradiation is not required to induce a bystander effect in normal human keratinocytes: evidence for release during irradiation of a signal controlling survival into the medium. Radiat Res 1998;149:256–262. [PubMed: 9496888]
50. Weaver VM, Petersen OW, Wang F, Larabell CA, Briand P, Damsky C, Bissell MJ. Reversion of the malignant phenotype of human breast cells in three-dimensional culture and in vivo by integrin blocking antibodies. J Cell Biol 1997;137:231–245. [PubMed: 9105051]
51. Pinto M, Howell RW. Concomitant quantification of targeted drug delivery and biological response in individual cells. Biotechniques 2007;43:64–71. [PubMed: 17695254]
52. Pandey BN, Gordon DM, de Toledo SM, Pain D, Azzam EI. Normal human fibroblasts exposed to high- or low-dose ionizing radiation: differential effects on mitochondrial protein import and membrane potential. Antioxid Redox Signal 2006;8:1253–1261. [PubMed: 16910773]
53. Bagley J, Rosenzweig M, Marks DF, Pykett MJ. Extended culture of multipotent hematopoietic progenitors without cytokine augmentation in a novel three-dimensional device. Exp Hematol 1999;27:496–504. [PubMed: 10089912]
54. Wersto RP, Chrest FJ, Leary JF, Morris C, Stetler-Stevenson MA, Gabrielson E. Doublet discrimination in DNA cell-cycle analysis. Cytometry 2001;46:296–306. [PubMed: 11746105]
55. Bishayee A, Rao DV, Howell RW. Evidence for pronounced bystander effects caused by nonuniform distributions of radioactivity using a novel three-dimensional tissue culture model. Radiat Res 1999;152:88–97. [PubMed: 10428683]
56. Eckerman, KF.; Endo, A. MIRD: Radionuclide Data and Decay Schemes. Society of Nuclear Medicine; Reston, VA: 2008.
57. Howell RW, Goddu SM, Rao DV. Design and performance characteristics of an experimental cesium-137 irradiator to simulate internal radionuclide dose rate patterns. J Nucl Med 1997;38:727–731. [PubMed: 9170437]
58. Schutte B, Reynders MM, van Assche CL, Hupperets PS, Bosman FT, Blijham GH. An improved method for the immunocytochemical detection of bromodeoxyuridine labeled nuclei using flow cytometry. Cytometry 1987;8:372–376. [PubMed: 3113895]
59. Fenech M, Chang WP, Kirsch-Volders M, Holland N, Bonassi S, Zeiger E. HUMN project: detailed description of the scoring criteria for the cytokinesis-block micronucleus assay using isolated human lymphocyte cultures. Mutat Res 2003;534:65–75. [PubMed: 12504755]

60. Neti PV, Howell RW. Log normal distribution of cellular uptake of radioactivity: implications for biologic responses to radiopharmaceuticals. J Nucl Med 2006;47:1049–1058. [PubMed: 16741316]

61. Mitchell JB, Russo A, Cook JA, Straus KL, Glatstein E. Radiobiology and clinical application of halogenated pyrimidine radiosensitizers. Int J Radiat Biol 1989;56:827–836. [PubMed: 2573682]

62. Bishayee A, Hill HZ, Stein D, Rao DV, Howell RW. Free radical-initiated and gap junction-mediated bystander effect due to nonuniform distribution of incorporated radioactivity in a three-dimensional tissue culture model. Radiat Res 2001;155:335–344. [PubMed: 11175669]

63. Nagasawa H, Little JB. Unexpected sensitivity to the induction of mutations by very low doses of alpha-particle radiation: evidence for a bystander effect. Radiat Res 1999;152:552–557. [PubMed: 10521933]

64. Schettino G, Folkard M, Michael BD, Prise KM. Low-dose binary behavior of bystander cell killing after microbeam irradiation of a single cell with focused C_k X rays. Radiat Res 2005;163:332–336. [PubMed: 15733040]

65. de Toledo SM, Asaad N, Venkatachalam P, Li L, Howell RW, Spitz DR, Azzam EI. Adaptive responses to low-dose/low-dose-rate gamma rays in normal human fibroblasts: the role of growth architecture and oxidative metabolism. Radiat Res 2006;166:849–857. [PubMed: 17149977]

66. Azzam EI, de Toledo SM, Little JB. Expression of CONNEXIN43 is highly sensitive to ionizing radiation and other environmental stresses. Cancer Res 2003;63:7128–7135. [PubMed: 14612506]

67. Zhou H, Randers-Pehrson G, Suzuki M, Waldren CA, Hei TK. Genotoxic damage in non-irradiated cells: contribution from the bystander effect. Radiat Prot Dosimetry 2002;99:227–232. [PubMed: 12194291]

68. Mitchell SA, Randers-Pehrson G, Brenner DJ, Hall EJ. The bystander response in C3H 10T½ cells: the influence of cell-to-cell contact. Radiat Res 2004;161:397–401. [PubMed: 15038773]

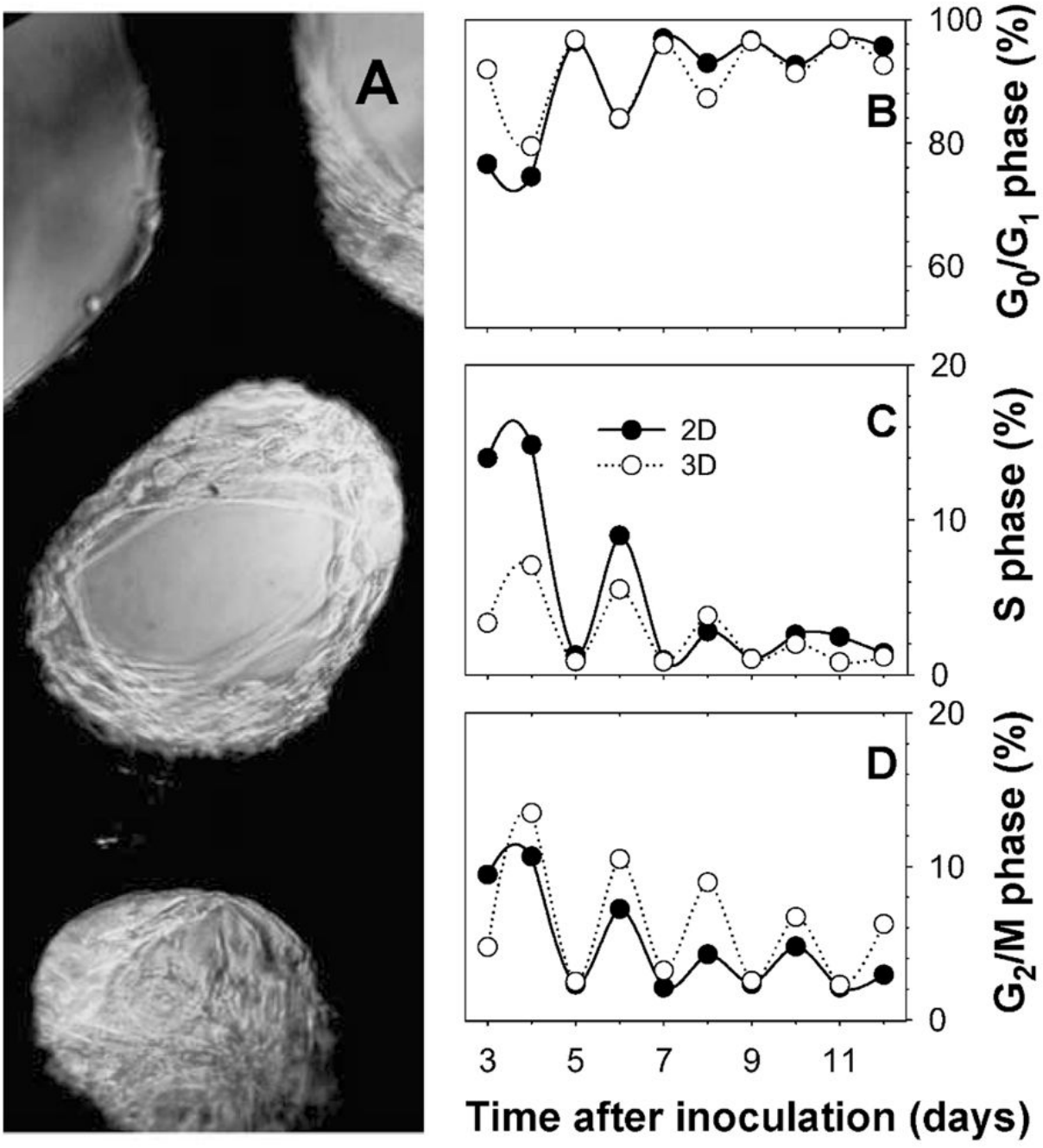

FIG. 1.

Characterization of the Cytomatrix™ 3D culture model. Panel A: AG1522 fibroblasts adapted to grow in 3D on Cytomatrix™ units, which appear dark in bright-field microscopy. Panels B, C and D: cMEM feeding regimen determines the cell cycle distribution and therefore the fraction of cells that may be targeted via pulse labeling with ^{3}HdC. G_0/G_1- (panel B), S- (panel C), and G_2/M-phase fractions (panel D) were measured as function of time after inoculation with cells in 2D (●) or 3D Cytomatrix™ (○) cultures. Cultures were fed with cMEM on odd-numbered days after inoculation.

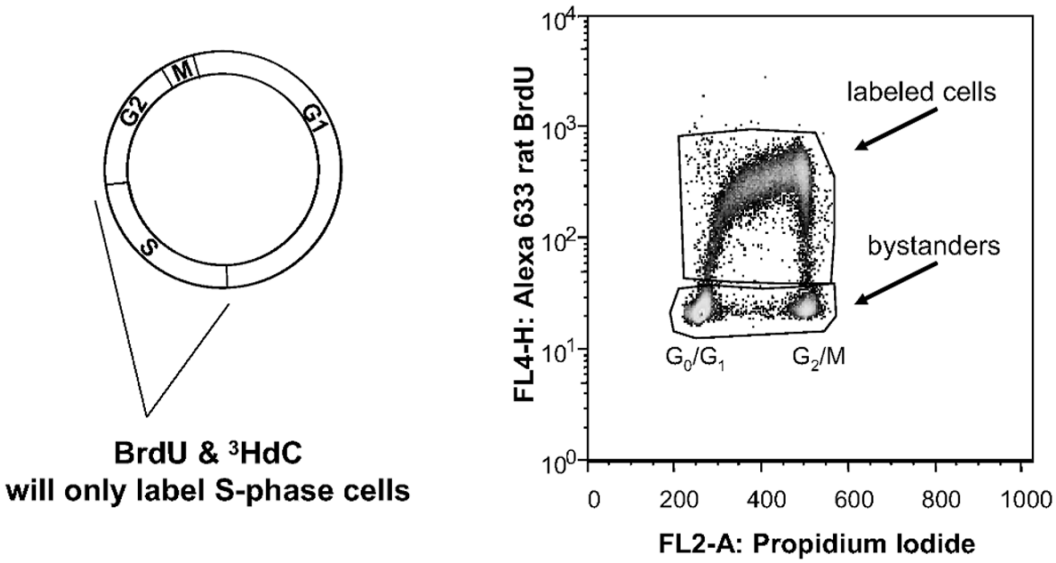

FIG. 2.

Strategy for labeling a small fraction of the cell population with ^{3}HdC in a manner that allows identification of the labeled cells with flow cytometry. Left: Cells are pulse labeled for 3 h with a cocktail of ^{3}HdC and BrdU. Only cells that enter or are in S phase during the pulse-labeling period incorporate ^{3}HdC and BrdU into their DNA. Right: Flow cytometry dot plot showing $BrdU^{+}$ (labeled) and $BrdU^{-}$ (bystander) cells. The ordinate represents fluorescence intensity associated with BrdU (and ^{3}HdC) incorporation, whereas the abscissa represents fluorescence from PI, which is a measure of DNA content. The G_0/G_1-phase and G_2/M-phase populations are denoted. S-phase cells are found at intermediate values of PI fluorescence intensity.

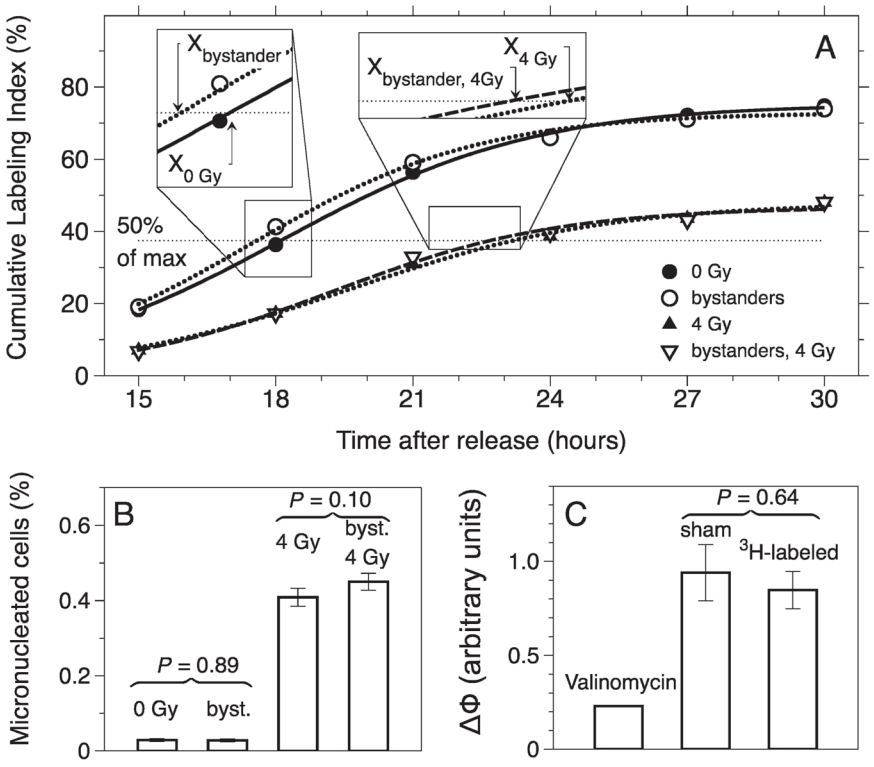

FIG. 3.

Analyses of stress responses in bystander cells. Panel A: Cumulative labeling index of bystander cells cocultured on the Cytomatrix™ with ^{3}HdC labeled cells and for the same bystander cells that later received a 4-Gy challenge dose with γ rays. Curves indicate sigmoid regressions. The half-rise times, $X_{bystanders}$ and $X_{0\ Gy}$, for bystander and unchallenged cells, respectively, are shown on the *x* axis along with estimates of $X_{bystanders,\ 4\ Gy}$ and $X_{4\ Gy}$. Panel B: Induction of micronuclei in bystander cells and bystander cells that were later subjected to a 4-Gy challenge with γ rays. Panel C: Shift in mitochondrial membrane potential after exposure to 4 Gy γ radiation 24 h after pulse labeling with ^{3}HdC.

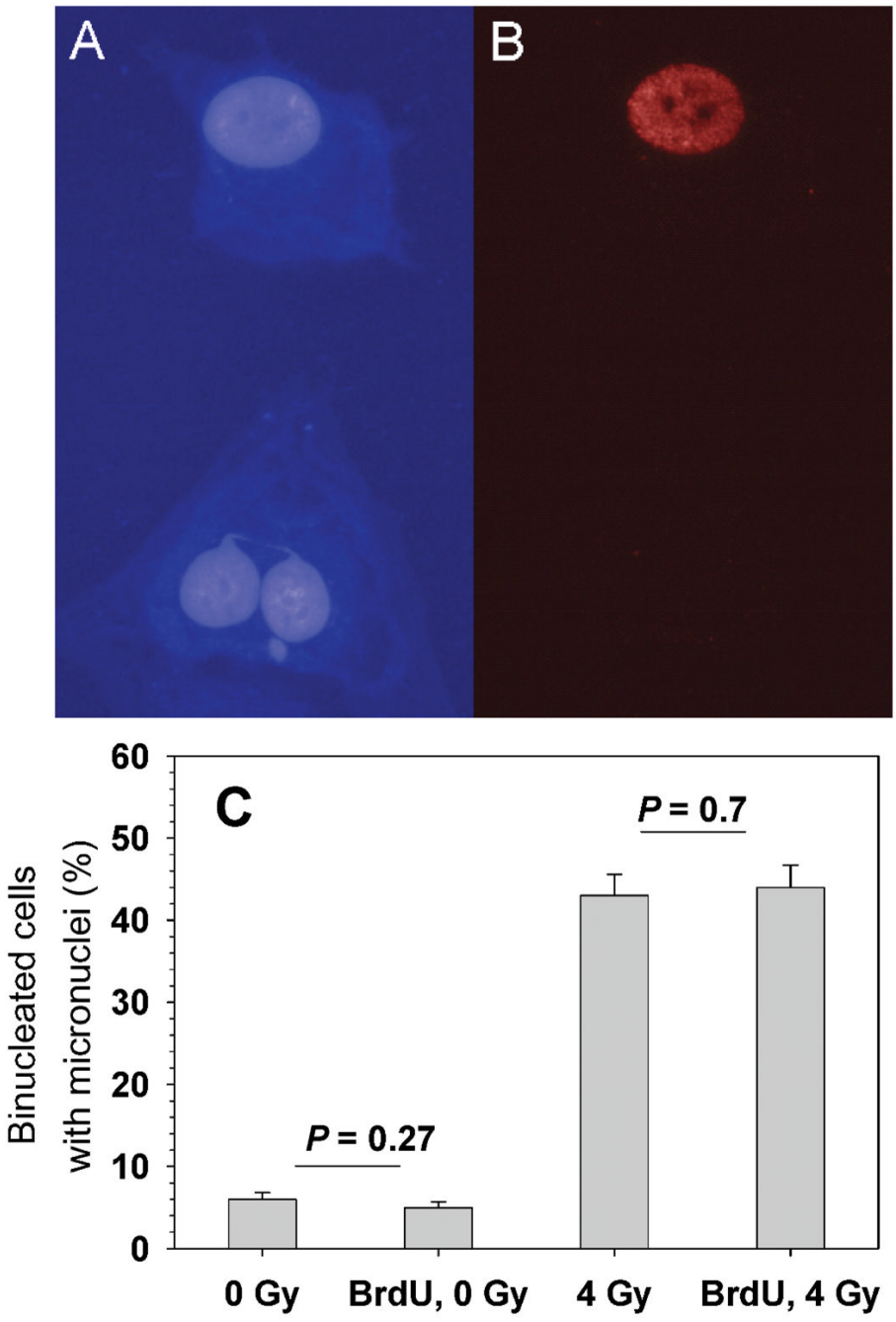

FIG. 4.

Induction of DNA damage in bystander cells (not labeled with ^{3}HdC). Panel A: Hoechst staining of DNA. Panel B: BrdU immunostaining. The images show a bystander cell (unlabeled) with a micronucleus and a nucleoplasmic bridge (bottom) along with a radiolabeled ($BrdU^{+}$) cell with no micronuclei (top). Panel C: Micronucleus frequencies in bystander cells in the absence or presence of BrdU in the ^{3}HdC-labeled cells and in the absence or presence of a 4-Gy challenge dose of γ rays. Background micronucleus frequencies in sham-labeled and sham-irradiated samples varied from 2% to 5% in different experiments (see also Table 2).

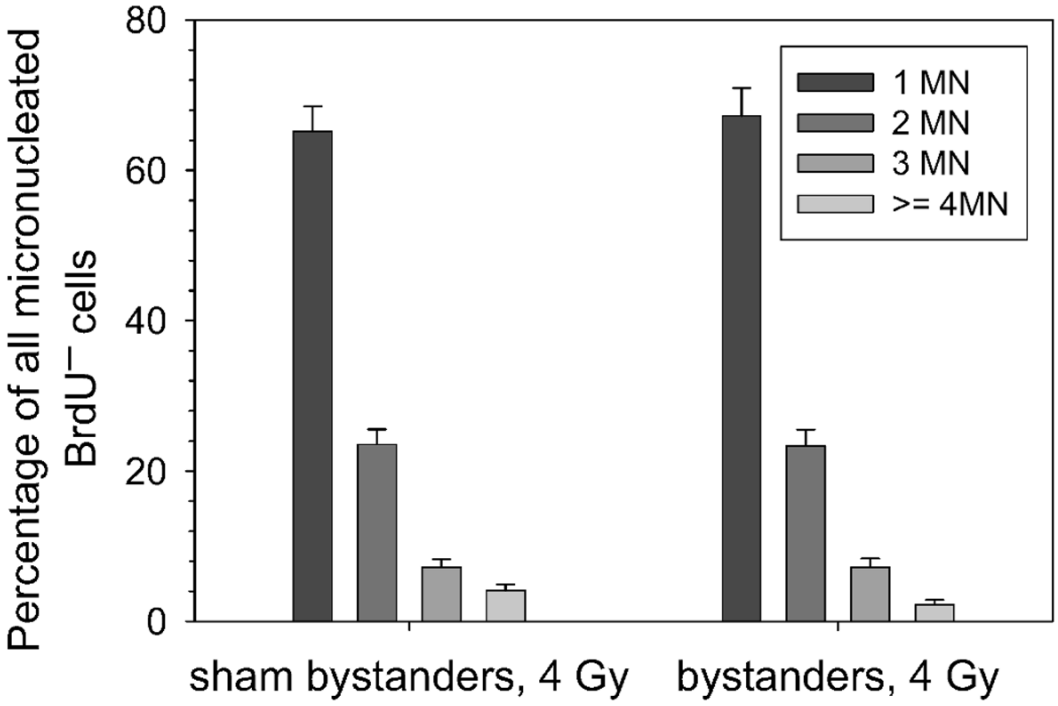

FIG. 5.

Frequency of micronuclei in bystander cells (unlabeled) that were cocultured with either ^{3}HdC or with sham-labeled cells, then challenged with 4 Gy γ radiation. Error bars were drawn assuming Poisson statistics for the measured frequencies.

TABLE 1

Results of Sigmoid Regression Analysis on Individual FCM-CLI Experiments, Grouped by Hours of Coculture in 3D

Experiment ID	$X_{0\ Gy}$ (hours)	$X_{bystanders}$ (hours)	$X_{4\ Gy}$ (hours)	$X_{bystanders,\ 4\ Gy}$ (hours)	Cells labeled (%)	Activity per labeled cell (mBq/cell)	Dose rate to labeled cells (mGy/h)
3 h coculture							
^{3}HdC15	19.1	19.3			3	16	235
^{3}HdC15b	19.1	19.5			3	3.1	45
^{3}HdC18	18.4	18.0	22.4	21.2	16	7.1	104
^{3}HdC 20	18.3	17.0	25.6	24.0	16	4.8	70
^{3}HdC21	17.1	17.9	29.5	23.4	2	7.8	114
^{3}HdC24	22	20	27.3	23.2	2	17	250
^{3}HdC25	18.0	16.9	23.7	22.4	2	25	370
^{3}HdC26	18.1	17.5	23.4	24.9	5	4.5	66
^{3}HdC27	17.7	17.3	24.0	22.3	2	13	191
^{3}HdC28	18.1	17.6	23.3	22.8	2.4	11	161
^{3}HdC29	17.4	17.4	22.8	25.6	1.8	10	14.7
8 h coculture							
^{3}HdC12	18	19			7	2	29
^{3}HdC12b	18	17			7	13	190
^{3}HdC13	18	18			3	2.9	42
^{3}HdC13b	18	17			3	19	280
24 h coculture							
^{3}HdC31	18.0	18.1			1.7	12.3	180
^{3}HdC32	19.0	19.0			3.5	10.8	160
^{3}HdC36	19.3	18.9	25.2	25.2	3	5.3	78
^{3}HdC37	20.3	20.7	24.9	23.7	2	4.5	66
^{3}HdC38	19.5	20.4	24.6	22.9	2	10	14.7
52 h coculture							
^{3}HdC16	20.6	20.3			3.7	3.4	50
^{3}HdC16	20.6	20.2			3.7	13.6	200

Note. For each experiment, the percentage of cells labeled and the average dose rate to the labeled cells are indicated.

TABLE 2

Pearson's χ^2 Tests on Results of Micronucleus Experiments with Bystander Cells ($BrdU^-$)

	Bystanders		Sham bystanders		
Experiment ID	**Binucleates scored**	**MN frequency**	**Binucleates scored**	**MN frequency**	***P* value**
^{3}HdC21*	2012	0.028 ± 0.004	2035	0.028 ± 0.004	0.89
^{3}HdC24	993	0.056 ± 0.007	990	0.038 ± 0.006	0.06
^{3}HdC25	1990	0.036 ± 0.004	1997	0.031 ± 0.004	0.37
^{3}HdC27	1468	0.044 ± 0.005	1998	0.028 ± 0.004	*0.01*
^{3}HdC31	1842	0.029 ± 0.004	1955	0.024 ± 0.003	0.31
^{3}HdC32	1988	0.023 ± 0.003	2008	0.022 ± 0.003	0.88
	Bystanders, 4 Gy γ rays		Sham bystanders, 4 Gy γ rays		*P* value
^{3}HdC24	623	0.43 ± 0.03	656	0.52 ± 0.03	*0.0007*
^{3}HdC25	994	0.50 ± 0.02	1266	0.46 ± 0.02	0.052
^{3}HdC27	174	0.54 ± 0.05	684	0.45 ± 0.03	*0.03*

Notes. Micronucleus frequencies were compared in bystander and sham bystander cultures, as well as in bystanders and sham bystanders that were challenged with 4 Gy γ radiation to test for adaptive bystander effects. Statistical significance is α = 0.05. Data sets marked with * are plotted in Fig. 3B.

TABLE 3

Measurements of Mitochondrial Membrane Potential to Assess the Involvement of Oxidative Metabolism in the Adaptive Bystander Effect Measured by G_1 Arrest[a]

	JC1 probe fluorescence shift (arbitrary units)		
Experiment ID	**Sham-labeled cultures**	**^{3}HdC-labeled cultures**	***P* value**
^{3}HdC30	0.68 ± 0.09	0.94 ± 0.09	*0.016*
^{3}HdC31	0.64 ± 0.01	0.63 ± 0.01	0.57
^{3}HdC32	0.53 ± 0.01	0.50 ± 0.01	*0.04*
^{3}HdC36	0.96 ± 0.06	1.1 ± 0.1	0.29
^{3}HdC37	0.58 ± 0.08	0.6 ± 0.1	0.89
^{3}HdC38*	0.9 ± 0.1	0.8 ± 0.1	0.64

Notes. P values are from Student's *t* test. Statistical significance is $\alpha = 0.05$. Data sets marked with * are plotted in Fig. 3C.

[a] See also Table 1.